sustainability

MDPI

Article

Rheology, Mechanical Properties and Shrinkage of Self-Compacting Concrete Containing Cement Kiln and By-Pass Filter Dust

Andreas Kounadis [1], Efstratios Badogiannis [1,*], Kosmas Sideris [2], Stelios Antiohos [3] and Ioannis Marinos [3]

[1] School of Civil Engineering, NTUA, GR-15773 Zografou, Greece; andkoun@yahoo.gr
[2] School of Civil Engineering, DUTH, GR-69100 Xanthi, Greece; kksider@civil.duth.gr
[3] TITAN Cement Company S.A., GR-11143 Athens, Greece; s.antiochos@titan.gr (S.A.); marinosi@titan.gr (I.M.)
* Correspondence: badstrat@central.ntua.gr; Tel.: +30-210-772-1266

Abstract: Self-compacting concrete (SCC) is a high-quality construction solution, combining high fluidity, passing and filling ability with improved mechanical properties and durability. In the present study, the effect of incorporating alternative waste materials, such as two by-products of the cement industry, namely cement kiln dust (CKD) and by-pass dust (BPD) into SCC, as a partial replacement for traditional filler material, was investigated. The produced compositions were compared with reference mixtures containing exclusively marble powder (MP), as a filler. A series of tests encompassing specific test methods for wet SCC, compressive, flexural and tensile-splitting strength tests, as well as drying-shrinkage determination, were undertaken to evaluate the quality of the produced SCC in terms of fresh and hardened properties. The use of alternative fine-filler materials resulted in a high-performance sustainable SCC, of low cement content. To be precise, incorporating CKD into the SCC enhanced its rheological behavior and marginally improved its mechanical properties, while the use of BPD led to SCC mixtures of adequate rheological characteristics, coupled with significantly improved mechanical and physical properties.

Keywords: self-compacting concrete; fine-filler material; rheology; compressive strength; drying shrinkage

check for updates

Citation: Kounadis, A.; Badogiannis, E.; Sideris, K.; Antiohos, S.; Marinos, I. Rheology, Mechanical Properties and Shrinkage of Self-Compacting Concrete Containing Cement Kiln and By-Pass Filter Dust. *Sustainability* **2024**, *16*, 320. https://doi.org/10.3390/su16010320

Academic Editor: Ramadhansyah Putra Jaya

Received: 18 November 2023
Revised: 22 December 2023
Accepted: 25 December 2023
Published: 29 December 2023

1. Introduction

In 1983 in Japan, the constructions showed high intensity problems of durability, due to the incomplete or excessive consolidation of the concrete. As a solution, in 1986, Okamura introduced the self-compacting concrete (SCC), distinguished by its essential ability of being compacted under its own weight, without any mechanical or human effort [1–3]. To attain its enhanced properties, such as the high filling and passing ability, specific modifications in the mix design of the composition of SCC are required, compared to the conventional vibrated concrete (VC) [2,4]. The most widely embraced changes are related to the addition of modern active chemical admixtures and fine-grained fillers, in appropriate proportions. The chemical admixtures mostly used are superplasticizers (SPs), which provide the mixture with high fluidity by decreasing the yield stress, and viscosity-modifying agents (VMAs), which increase the robustness and the viscosity of the mixture [5]. Fillers are added to the composition to mitigate segregation and improve the microstructure of the concrete by optimizing the packing of the dry ingredients (namely, cement and aggregates) [6–9]. An important subject of scientific research is the type of filler, with parameters such as size, shape and chemical composition emerging as the most critical. A rising number of research teams are trying to use industrial by-products as fillers, aiming to promote sustainability and greener constructions by utilizing materials that would potentially be air or soil pollutants [7,10–16]. When it comes to cement plants, especially, thousands of tons of waste material are amassed annually, making the need for their purposeful utilization imperative. In more detail, during the continuous feeding of kilns with raw materials for clinker production, large quantities of fine-grained material are trapped in the gases and removed by control devices, such as cyclones, bag houses or electrostatic filters [17,18]. Their incorporation into concrete to partially replace cement or conventional fillers (such as limestone dust or marble powder) constitutes a topic of increasing interest.

Wang et al., 2018 [19], claimed that the addition of limestone filler to concrete can either have a positive or negative effect on the workability, depending on the incorporation proportion, the particle size in comparison to the corresponding cement particles, or the MgO content; the increase in which enhances the viscosity of concrete. An increase in limestone powder may cause a decrease in the compressive strength of concrete, due to the dilution effect of a high filler content; however, at an optimum amount and size it can create a closer packing of the dry materials, and thus increase the compressive strength. Limestone filler is considered to be a material of higher stiffness compared to concrete, which leads to a higher modulus of elasticity. Elyamani et al., 2014 [6], compared the effect of different fillers on the rheological and mechanical properties of SCC. The non-pozzolanic fillers, such as marble dust, alleviated the phenomena of bleeding and segregation compared to pozzolanic fillers, such as silica fume and metakaolin, while the presence of marble dust decreased the water absorption. No substantial changes in compressive strength were noted when comparing pozzolanic to non-pozzolanic fillers. However, the latter, despite not participating in hydration reactions, enhanced the microstructure of the cement paste, exerting a positive influence on both the bulk paste matrix and the transition zone. Sfikas et al., 2014 [20], investigated the partial replacement of limestone filler or cement with metakaolin resulting in a higher demand for chemical admixtures, as the ratio of metakaolin to limestone powder or cement increased, due to the higher specific surface area and the non-spherical shape of metakaolin particles.

Abukhashaba et al., 2014 [21], used cement kiln dust (CKD) in fiber-reinforced SCC, and produced a sustainable SCC. However, due to the physical properties of CKD, a higher demand of SP dosages is required to achieve the desired rheological behavior. Siddique et al., 2006 [22], claimed that the incorporation of CKD into concrete in an appropriate amount can have a positive effect on sorptivity and alkali–silica reactions, while it does not appear to adversely affect properties such as the compressive and flexural strengths. Bagheri et al., 2020 [23], used CKD and fly ash in different proportions (0–40% and 0–30%, respectively) to produce a green concrete with improved fresh and hardened properties. Replacing 20% of cement with 5% of CKD and 15% of fly ash led to a higher compressive strength, while for mixtures with 20% or higher CKD the compressive strength decreased sharply. Maslehuddin et al., 2009 [24], also investigated the mechanical properties and durability of concrete containing 0–15% CKD. Increasing CKD decreased the compressive strength of the concrete. However, with a 5% replacement of cement with CKD, there was no significant impact on compressive strength or drying shrinkage. Najim et al., 2014 [25], claim that the compressive strength decrease due to CKD incorporation could mainly be detected in cases of CKD with high free-lime content, as free lime reacts with water and produces additional $Ca(OH)_2$, resulting in pores of higher volume and subsequently greater internal stresses, leading to modified cementitious mortars of decreased compressive strength.

Viacava et al., 2012 [26], produced medium-strength SCC by replacing cement with CKD at ratios of 20% and 30%. They concluded that replacing cement with CKD improves the rheological properties effectively, reducing the use of chemical admixtures. Specifically, 20% replacement of cement with CKD led to a lower segregation tendency and higher viscosity, as observed through segregation and a V-funnel test, respectively.

Ashteyat et al., 2018 [27], produced five SCC compositions by replacing 0–25% cement with white cement by-pass dust (BPD), without facing any problem in terms of workability. Even when the compressive strength was sufficient, a scalable, according to BPD content, reduction occurred. The drying shrinkage, as well as capillary porosity measurements, showed a slight increase, due to the incorporation of BPD. The porosity decreased when replacing 10% of cement with BPD, while the most encouraging result concerned the SCC resistance to the alkali–silica reaction.

In almost all the aforementioned studies, a common approach is found for the mix design process, considering the specific by-products of clinker processing as supplementary cementitious materials (SCMs) and replacing cement in various percentages. Moreover, in most of these research endeavors, the substitution of cement with CKD or BPD did not yield the anticipated improvement in mechanical properties; instead, a degradation was commonly observed. Therefore, it is imperative to explore alternative approaches for incorporating CKD or BPD. Thus, the purpose of this paper is to investigate the possibility of utilizing these two raw by-products of the cement industry, cement kiln dust (CKD) and by-pass dust (BPD), as fine-filler materials of SCC, in comparison with a reference mixture containing only marble powder (MP), by designing two series of SCC mixtures of dissimilar water-to-cement ratio and filler content. The properties and the characteristics of CKD and BPD are governed by the clinker raw materials and the kilns' layout details, such as the fuels and filters used. Therefore, the quality and the suitability of similar by-products for further use in the building sector should be evaluated by taking into consideration the specific process characteristics of each cement production plant. After the characterization of the fillers in terms of chemical composition, skeletal density and particle size distribution, compositions of concrete of high water-to-cement ratio and low cement content were produced. Properties of fresh and hardened concrete were studied. The analysis of the results of the rheological and mechanical properties demonstrated a high potential for utilizing the examined by-products for sustainable SCC compositions. Besides, ongoing research is focused on investigating the durability aspects [28], conducting microstructural analyses, and assessing the potential synergies in incorporating alternative fine-filler materials (CKD and BPD), alongside SCMs.

2. Experimental

2.1. Materials

Three nominal grades of locally crushed calcareous limestone aggregate, in accordance with EN 12620:2013 [29], were used as follows: sand 0/4 mm, small gravel (g1) 0/8 mm and medium gravel (g2) 0/16 mm. Portland cement CEM I 42.5R, conforming to EN 197-1:2011 [30], and tap water (pH = 7, 20 °C) were used. Two aqueous solutions, a viscosity modifying agent (VMA), based on a synthetic copolymer of low viscosity with extremely efficient rheological properties, and a superplasticizer (SP) based on modified polymers, both complying with EN 934-2 [31], were used in appropriate proportions to provide the SCC mixtures with the desirable yield stress, viscosity and robustness.

The behavior of three fine-filler materials in concrete mixtures was investigated, namely marble powder (MP), a by-product from marble processing, cement kiln dust (CKD) and by-pass dust (BPD), which constitute by-products of the clinker production process.

Details about physical and chemical properties, as well as particle size distribution are presented in Table 1, Table 2 and Figure 1, respectively, and have been experimentally defined and presented by the authors in earlier studies [32]. In more detail, regarding the methodologies employed, specific gravity of the cement powder and fine-filler materials was defined in accordance with ASTM B923-02 [33] via helium pycnometry, while their particle size distribution and specific surface area were determined in accordance with ISO 13320 [34], via laser diffraction particle-size analysis, by measuring the scattering angle and the intensity of the light scattered on the particles. The X-ray diffraction method (XRD) was employed to determine the mineralogical characteristics of the used filler materials. As MP primarily contains calcite, only the results for CKD and BPD are illustrated in Figure 2. In more detail, CKD contains calcite, quartz, dolomite, albite, kaolinite, illite, and sylvite, as well as a high value of LOI, which is attributed to the $CaCO_3$ decomposition. BPD contains lime, and a mineral phase that encompasses SO_4^{2-}, alkalis and Cl^-, like anhydrite, sanidine and sylvite. Traces of clinkers' mineral phases, mainly C_2S, are also present. It is worth mentioning that the chemical composition of CKD and BPD may differ significantly from one plant to another, due to variations in raw materials and fuels. Table 1 exclusively presents information pertaining to the specific batch of by-products obtained from a particular cement plant (Kamari cement plant). The XRD of the cement powder is also presented in Figure 3.

Table 1. Physical properties of the fine materials used.

Property and Size Characteristics	Cement	MP	CKD	BPD
Specific Gravity (kg/m^3)	3150	2700	2700	2800
Specific Surface Area (cm^2/g)	3470	12,700	25,000	5000
d10 (μm)	4.74	1.44	1.13	12.95
d50 (μm)	19.82	4.88	3.71	50.72
d90 (μm)	57.41	12.27	14.66	115.63

Table 2. Chemical analysis (*w*/*w* %) of the fine materials used.

Compound (%)	Cement	MP	CKD	BPD
SiO_2	19.02	0.35	10.18	19.39
Al_2O_3	4.59	-	3.64	5.13
Fe_2O_3	3.63	0.07	2.06	3.46
CaO	63.43	55.41	43.53	52.73
MgO	2.02	0.76	1.31	2.22
MnO	-	0.01	-	-
SO_3	3.48	-	1.18	6.73
K_2O	0.47	-	1.71	4.84
Na_2O	0.28	-	0.37	0.46
P_2O_5	0.17	-	-	-
TiO_2	0.28	-	-	-
Cl	-	-	0.35	2.16
Loss of Ignition (LOI)	2.62	43.4	35.65	2.88

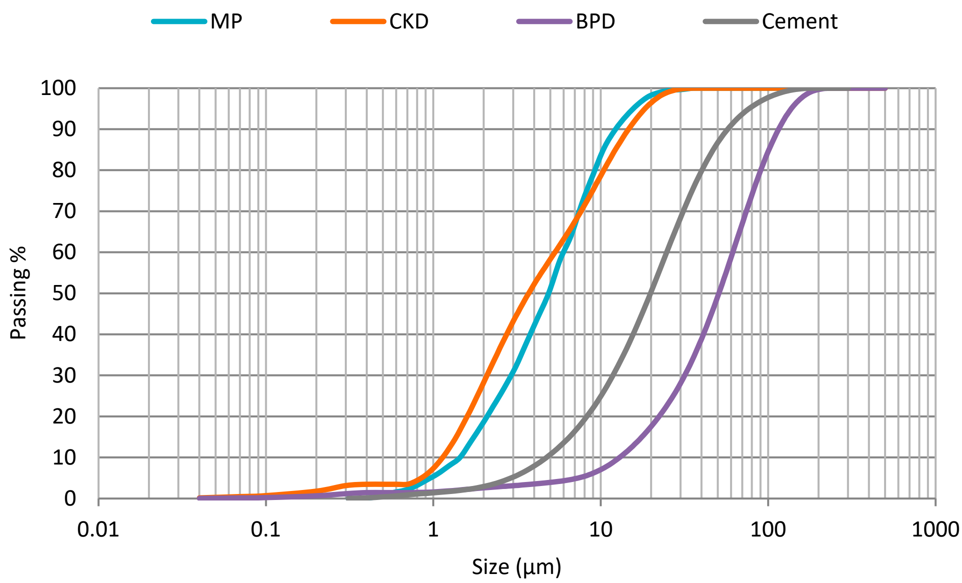

Figure 1. Particle size distribution of fine materials used.

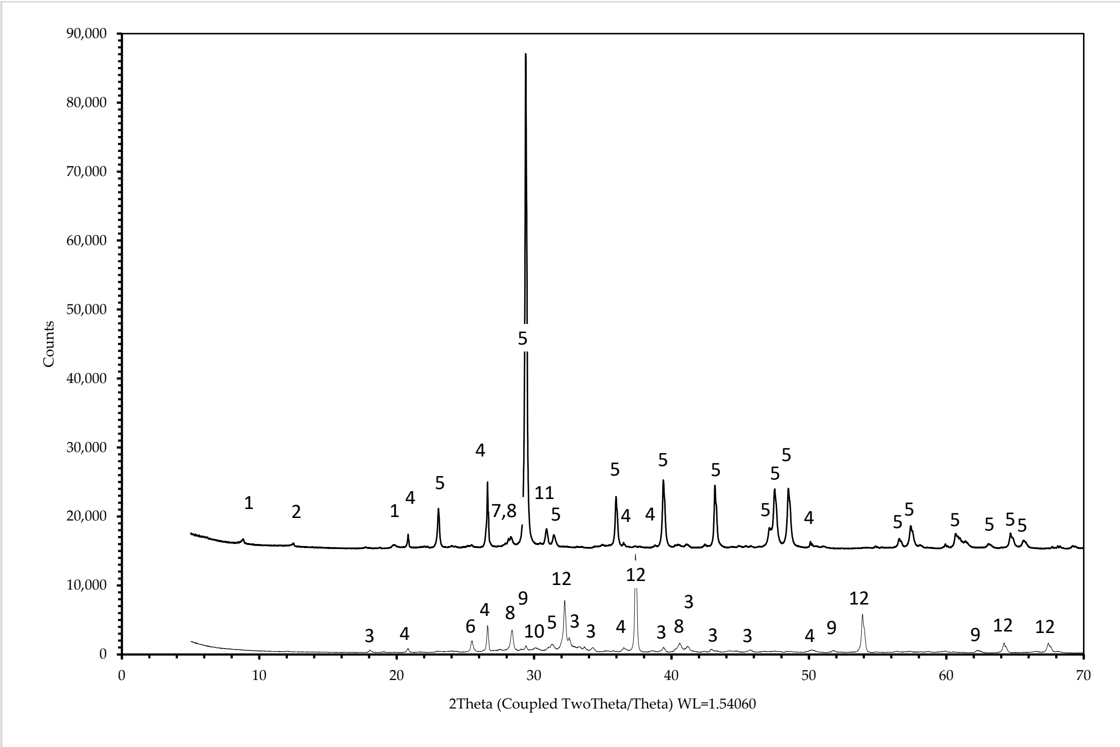

Figure 2. XRD patterns of CKD (top) and BPD (bottom): 1. Illite (ICCD 02-0056) 2. Kaolinite (ICCD 03-0058) 3. Larnite (ICCD 70-0388) 4. Quartz (ICCD 33-1161) 5. Calcite (ICCD 05-0586) 6. Anhydrite (ICCD 72-0503) 7. Albite (ICCD 89-6423) 8. Sylvite (ICCD 04-0587) 9. C_3S (ICCD 73-0599) 10. Wollastonite (ICCD 72-2284) 11. Dolomite (ICCD 84-2065) 12. Lime (ICCD 78-0649).

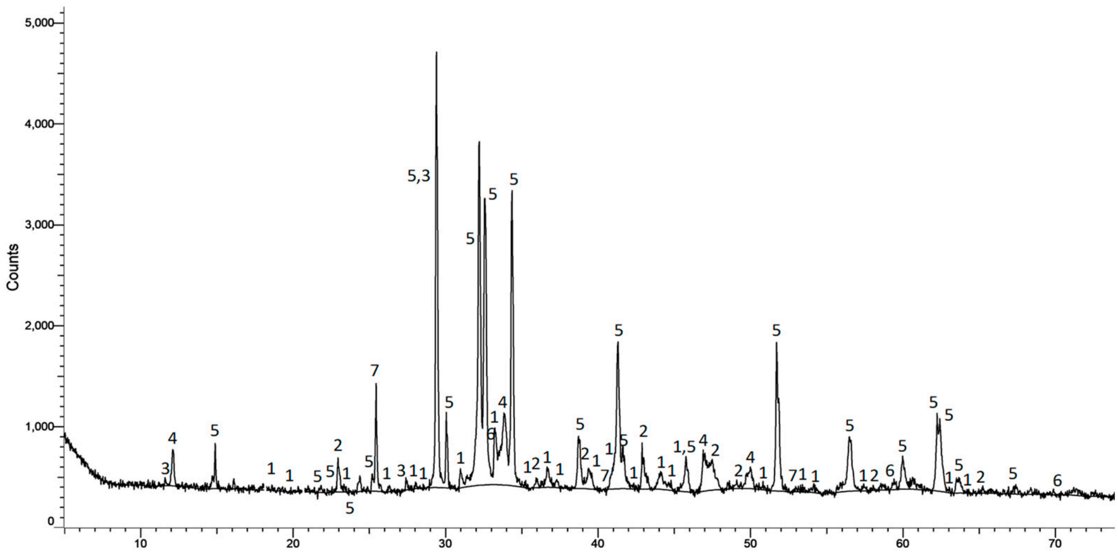

Figure 3. XRD patterns of cement: 1. C_2S (ICCD 70-0388) 2. Calcite (ICCD 05-0586) 3. Gypsum (ICCD 76-1746) 4. C_4AF (ICCD 70-2764) 5. C_3S (ICCD 73-0599) 6. C_3A (ICCD 32-0148) 7. Anhydrite (ICCD 37-1496).

2.2. Mix Design and Mixing Procedure

Three SCC mixtures were prepared with a constant active water-to-cement (w/c) and water-to-powder (w/p) ratio of 0.60 and 0.36, respectively. The reference mixture contained 200 kg/m^3 MP, of which 50% by weight was replaced by CKD and BPD, correspondingly, in the other compositions. All other SCC ingredients (cement, water, fine and coarse aggregates) remained the same as shown in Table 3. The marginally acceptable, or even unacceptable in some cases, rheological results led to an additional series of compositions with a higher cement-paste-to-total-aggregate ratio. Specifically, the reference composition of the new series contained 50 kg/m^3 more MP and additional water, to retain the ratio of water-to-powder at 0.36, while the amount of cement content remained the same. Of the total 250 kg/m^3 of filler material, 150 kg/m^3 was replaced by BPD and CKD in the other two compositions. These compositions are also presented in detail in Table 3. In both composition series, the water-to-powder ratio was kept constant, for comparison.

Table 3. Ingredients' content (kg/m^3) in SCC compositions produced.

Mixture	Water	Cement	MP	CKD	BPD	Sand	g1	g2	w/c	w/p
REF1	180	300	200	0	0	900	560	240	0.60	0.36
CKD1	180	300	100	100	0	900	560	240	0.60	0.36
BPD1	180	300	100	0	100	900	560	240	0.60	0.36
REF2	198	300	250	0	0	900	525	225	0.66	0.36
CKD2	198	300	100	150	0	900	525	225	0.66	0.36
BPD2	198	300	100	0	150	900	525	225	0.66	0.36

A fixed-pan planetary-type concrete mixer with rotating blades of 100 L capacity was employed for meticulous mixing and the production of all batches. For each SCC composition, a mixture of 40 L was prepared, adhering to the following procedure. All dry ingredients (cement, filler material, fine and coarse aggregate) were introduced into the mixer, and were mixed for 60 s. Then, 80% of the total water was introduced and the mixture was mixed for an additional 180 s. Finally, the remaining 20% of the total water mixed with the initial SP dosage was added, and 60 s of mixing followed. For each extra dose of the chemical admixture (SP or VMA), an additional 60 s of mixing was conducted.

Steel molds were used for the casting of the concrete specimens, in the appropriate dimensions for each test. The specimens were demolded after 24 h, and were cured in water at 20 °C afterwards, until the testing age, which varied according to each test's specifications.

2.3. Testing

The rheological behavior of each mixture was investigated via a slump-flow test and a T500 test, V-funnel test, U-box and L-box test and sieve-segregation test, in accordance with EN 12350-8, EN 12350-9, EN12350-11, EN12350-10 and UNI 11044, respectively [35–39]. In addition, the wet density of SCC and the entrapped air content (pressure gauge method) were measured according to EN 12350-6 and EN 12350-7, respectively [40,41]. The SP dosage for each mixture was selected to reach a slump flow of 690–710 mm, while VMA was added whenever segregation signs were observed.

The compressive strength was measured according to EN 12390-3, at the ages of 7, 28 and 90 days (loading rate: 4.50 kN/s) [42]. At each testing age, three cubes of $100 \times 100 \times 100$ mm^3 were tested. A tensile splitting test and modulus-of-elasticity measurement conforming to the testing procedure of EN 12390-6 and ASTM C 469, respectively, were conducted [43,44]. Specifically, cylindrical specimens of radius of 100 mm and height of 200 mm were tested at the age of 90 days after casting. Four loading cycles were performed for each specimen for the measurement of the modulus of elasticity, the first of which was used for the stress redistribution procedure.

After splitting, the visual stability index (VSI) was determined by observing any signs of paste or mortar layer at the top of the specimens, or non-normal distribution of the aggregate sizes. Specifically, if no paste or mortar is observed on top of the cylinder, and there is no difference in the size and area percentage of coarse aggregates lengthwise, the stability of the SCC is ranked at 0, and the specimen is considered stable. If, however, there is a slight difference in the size or area percentage of the coarse aggregates lengthwise, yet still without any paste or mortar layer on top of the specimen, the SCC is categorized as 1 and stable. In cases where there is cement paste or a mortar layer on top of the specimen, despite the difference in the size distribution of the aggregates, the stability of the SCC is evaluated as 2 or 3, depending on the intensity of the phenomenon [45].

Prisms of 100 × 100 × 500 mm^3 were used for the measurement of drying shrinkage and mass loss at the age of 7, 14, 28 and 90 days, in accordance with EN 12390-16 (the age of 90 days instead of 56 days is selected in order to evaluate the effect of potential late-age reactivity of fine materials on drying shrinkage), while for the same prisms a flexural test was carried out at the age of 90 days, according to EN 12390-5 [46,47]. Indicative photos of the experimental procedures are shown in Figure 4.

Figure 4. Indicative photos of the experimental procedures for fresh and hardened SCC mixtures produced.

3. Results and Discussion

3.1. Rheological Properties

All measured properties of the fresh SCC are presented in Table 4. Given that all compositions were of SF2 class and of a specific slump-flow range of 690–710 mm, the SP dosage could be a critical factor for assessing the rheological behavior of each mixture and the way each filler affects the SCC's yield stress. On the other hand, VMA was added only to mixtures that showed a segregation tendency. BPD1 was the only composition where a VMA dosage of 0.3% was added, while this composition also demanded the highest percentage of SP (3.1%—approximately 80% higher than REF1) to achieve the desired slump-flow range. On the other hand, REF1 had the lowest SP demand of 1.7%, and is also characterized by the lowest viscosity regarding the series 1 compositions, which is indirectly shown by the correspondingly low V-funnel time of 12.7 s. BPD1 was the only mixture that exceeded the 25 s limit, while CKD1 could also be characterized by a high viscosity, as the evacuation time was measured at 22.8 s, although remaining within the acceptable range. The increase in viscosity due to the addition of BPD compared to the other fillers is also confirmed, with the highest time reaching a flow of 500 mm (T500), which accounts for 5.6 s. Nevertheless, in terms of T500 values, all mixtures of series 1 are classified in the VS2 viscosity class. The adverse effect of BPD on the rheology of concrete could be explained by the low roundness of BPD particles, which increases intergranular friction, as shown in images obtained by SEM [33]. Moreover, the high content of anhydrite and lime, in conjunction with alkalis and sulfates, also affected the rheology of the mixtures. They decreased the setting time of SCC, and subsequently degraded the workability indices, such as the yield stress and plastic viscosity, demanding higher SP doses [48,49]. What also contributes to the above in the cases of BPD and CKD, is the high content of K_2O (higher than Na_2O), which causes a significant acceleration in the hydration process [49]. To offset the rapid loss in workability due to a rapid hydration, a slower-reacting cement type or retarding chemical admixtures could be used [3].

Table 4. Fresh SCC test results and chemical admixtures needed for each SCC composition.

Mixture	SP/ Cement (%)	VMA/ Cement (%)	Unit Weight (kg/m^3)	Air Content (%)	Slump Flow (mm)	T500 (s)	V-Funnel (s)	U-Box -	L-Box -	Sieve Segregation (%)
REF1	1.7	-	2411	2.2	705	3.35	12.7	0.84	0.86	3.8
CKD1	2.4	-	2365	2.5	700	2.50	22.8	0.79	0.87	1.3
BPD1	3.1	0.3	2403	1.8	690	5.60	28.5	0.77	0.50	1.5
REF2	1.5	-	2256	2.9	690	1.59	5.1	0.93	0.88	7.5
CKD2	2.3	-	2264	3.3	695	1.07	3.6	0.89	0.90	8.0
BPD2	2.7	-	2358	1.5	700	2.82	15.3	0.78	0.71	2.2

As far as the sieve-segregation test results are concerned, all SCC mixtures of both series lie in the allowable range. The series 2 compositions show a slightly higher segregation vulnerability, compared to the corresponding compositions of series 1, but are not even approaching the 20% limit. This upward trend is clearly related to the higher water-to-powder and lower plastic viscosity, as indirectly determined by measuring the V-funnel evacuation time (Table 4). The different types of filler and demand in chemical admixture did not affect significantly the air content or fresh density of series 1, and in all mixtures these values fluctuated between 1.8% and 2.5%, and 2365 and 2411 kg/m^3, respectively [5]. Low deviations in unit weights, despite the difference in filler density, can be explained by the relatively low filler content. At the same time, when it comes to series 2 compositions, the lower unit weight could be attributed to the higher water content. The higher content of entrapped air in REF2 and CKD2 mixtures, which amounts to 2.9% and 3.3%, respectively, also contributes to the slightly reduced fresh density. Moreover, in series 2 mixtures, none of the compositions required a VMA dosage, while the BPD2 mixture required the highest amount of SP (2.7%) to achieve the desired slump-flow value. BPD2 showed the highest viscosity in terms of V-funnel time (15.3 s) and T500 (2.82 s), being, however, within the acceptable limits. Most SCCs of both series achieved acceptable results regarding the U-box and L-box, with the exception of the two compositions that contained BPD, which demonstrated a slightly low L-Box performance, with ratios of 0.50 and 0.71 for the two series, respectively. This could be due to the high plastic viscosity [3], as no signs of aggregate blockage were observed.

To analyze the rheological performance of the different mixtures, the values in Table 4 were normalized using the min–max normalization technique, by setting minimum and maximum values for each rheology parameter. In more detail, when the boundary limits of a property were available, they were applied (for instance, min value for slump flow, 660). Otherwise, specific limits have been defined for other indices (for instance, the limits of 0–5% w/w cement for the SP content). In essence, the ultimate limits are established to evaluate mixtures for increased success, denoting compositions that demand fewer chemical additives, thereby resulting in reduced air content, heightened resistance to segregation, and superior filling and passing ability, and fluidity, as well. With this technique, the evaluation base was common for all the rheological indices and, therefore, the rheological performance of the mixtures is compared by plotting a summary radar chart, shown in Figure 5. The highest values (exterior polygon vertices) indicate an optimum rheological behavior. According to the results depicted in Figure 5, REF2 and CKD2 exhibit nearly identical optimal behavior, demonstrating outstanding potential for self-leveling capabilities and excellent filling capacity, even in the presence of densely packed reinforcement [3].

On the other hand, BPD1 is the composition with the poorest performance in terms of fresh concrete properties, making its use restrictive for certain applications with high fluidity requirements. While its comparatively high viscosity may contribute beneficially to limiting formwork pressure, there is a risk of an undesirable thixotropic effect causing occasional stoppages or delays between successive lifts [3].

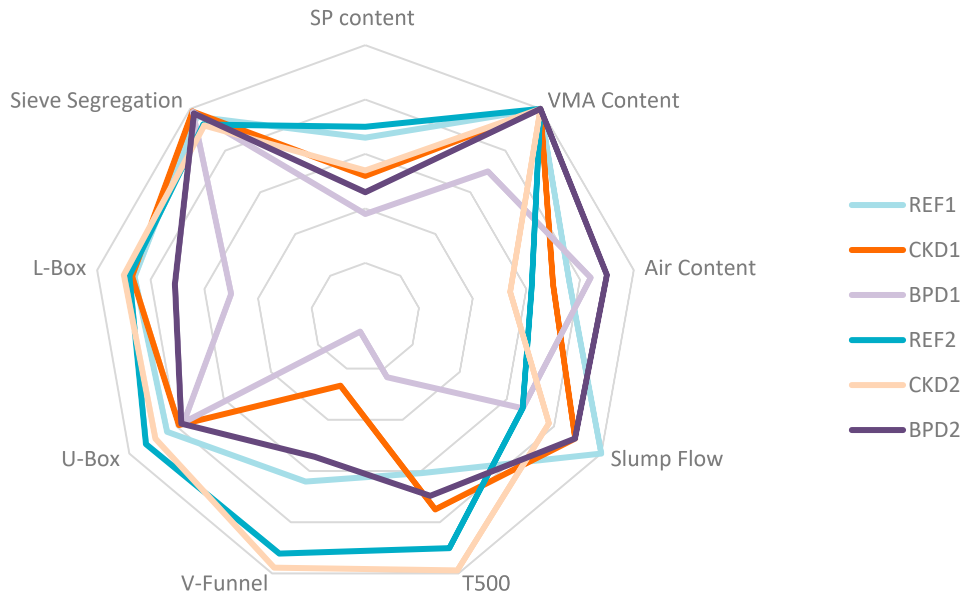

Figure 5. Chemical admixture consumption in relation to rheological performance indices of each SCC mixture.

3.2. Compressive Strength

In Figure 6, the compressive strength at 7, 28 and 90 days is illustrated for all six SCC compositions. Comparing the reference mixtures of the two series, it is observed that the compressive strength of REF1 at the age of 28 days is 26% higher than the corresponding strength of REF2. This is explained by the increase in the water-to-cement ratio (0.66, instead of 0.60). The high MP content (200 kg/m^3 and 250 kg/m^3, respectively), in conjunction with the low cement content of both reference compositions, led to a slightly decreased compressive strength, due to the dilution effect [50,51]. The BPD1 mixture at the ages of 7 and 28 days developed the highest strength (65.7 MPa and 73.3 MPa, respectively), while BPD2 was the composition with the highest compressive strength among the series 2 mixtures (49.0 and 60.7, respectively). The acceleration in the early-age strength could be partially explained by the presence of Cl^- (Table 2), which constitutes a well-known accelerator for the hydration of alite [52]. The high performance of SCC containing BPD can also be attributed to the presence of gypsum and anhydrate, which led to a faster hydration of C_3S and to the clinker mineral phases found in BPD (Figure 2) [48]. In addition, the high peak of hydration heat, mainly due to SO_3 presence, and the accelerated hydration process due to the presence of anhydrite, are also related to the development of higher compressive strength [32]. The high compressive strength is further enhanced by the low content of entrapped air in the BPD1 and BPD2 mixtures (1.8% and 1.5%, respectively), as shown in Table 4 and Figure 7. Moreover, according to Shoaib et al., 2000 [49], the high content of dust chlorides and sulphates yield chloro-aluminate and sulpho-aluminate hydrates, while the high alkali content of CKD tends to crystallize some hydration products. Both phenomena resulted in a hardened concrete matrix with a wider pore system. Nevertheless, in the studied SCC mixtures, an increase in compressive strength was observed, which is attributed to the physical action of CKD fine particles in conjunction with the relatively low content of SO_3, Cl^- and alkalis, as shown in Table 2. In other words, the physical action (filler effect) of CKD fine particles counteracts the negative effect of alkalis on the compressive strength, due to C_3S consumption [52].

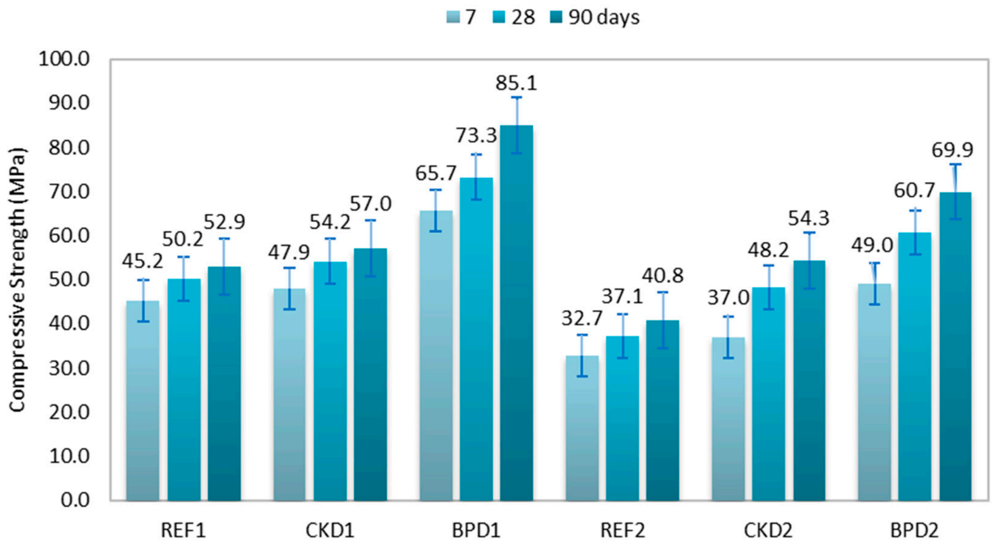

Figure 6. Compressive strength of each SCC composition at 7, 28 and 90 days.

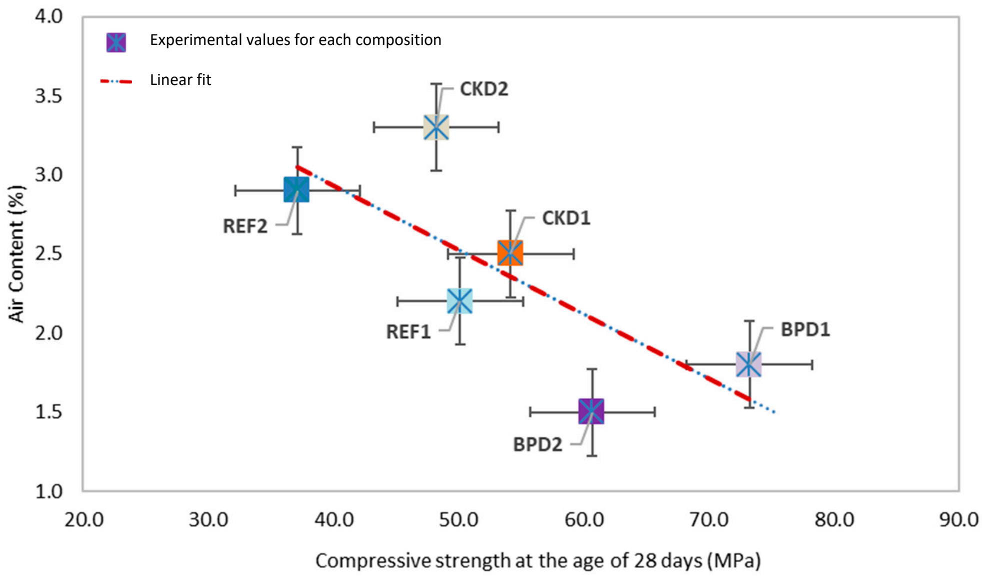

Figure 7. Correlation between the compressive strength (28 days) and the air content of the SCC mixtures.

At the age of 90 days, the compressive strength of the REF1 and REF2 compositions increased slightly, compared to that of 28 days, which indicates that MP is expectedly inactive in terms of pozzolanicity. Similarly, CKD illustrated a compressive strength increase from 28 to 90 days as low as 5% and 12.5%, for series 1 and series 2, respectively, and therefore it could also be considered as a material of low reactivity (inert or semi-inert) [3,26]. On the other hand, BPD contributed to late-hydration reactions, resulting in a high ratio of approximately 15% of 90-to-28 days compressive strength, for both series. The pozzolanic reactivity of BPD has also been confirmed by Singh et al., 1995 [53], after examining the consumption of calcium hydroxide obtained from the hydration of the cement paste. Moreover, according to the XRD analysis, BPD contains a comparatively higher amount of amorphous phases than that which is expected to react with calcium hydroxide at late ages, and this amount was probably totally consumed by the CH surplus at the late age of hydration [32].

Specifically, in Figure 7, the effect of the air content on compressive strength is understood in depth with the graphic illustration. As the void content increases, the compressive strength tends to decrease, while the above tendency deviates from the linearity given by the trendline depicted, due to factors related to the specific properties of the different fine-filler materials (videlicet, chemical, physical, and mechanical properties), as well as differences in the mix design of concrete [5,54].

3.3. Modulus of Elasticity

The moduli of elasticity for SCC compositions, as calculated from the stress—strain diagrams, are illustrated in Figure 8. All compositions were characterized by high values for the modulus of elasticity, possibly due to the high degree of MP content, an inert powder of higher hardness than that of cement paste, which fills the voids between the coarser aggregates and optimizes the packing density of the granular skeleton [19]. For the REF1, CKD1 and BPD1 compositions, the moduli of elasticity were calculated as being between 42.2–42.5 GPa at the age of 28 days, with negligible deviations observed among them. The moduli of elasticity of the CKD2 and BPD2 compositions were similar (36.6 GPa and 36.3 GPa, respectively), while the REF2 had the lowest modulus of elasticity (33.7 GPa), following a similar trend to that observed for the compressive strength. The lower moduli of elasticity of the series 2 specimens, in comparison with the corresponding ones of series 1, are attributed to the highest paste-to-aggregate and water-to-binder ratios [55]. It should be mentioned that the measurements of the elastic moduli were taken on water-saturated specimens, resulting in an approximately 15% increase in the results, compared to dry specimens [56].

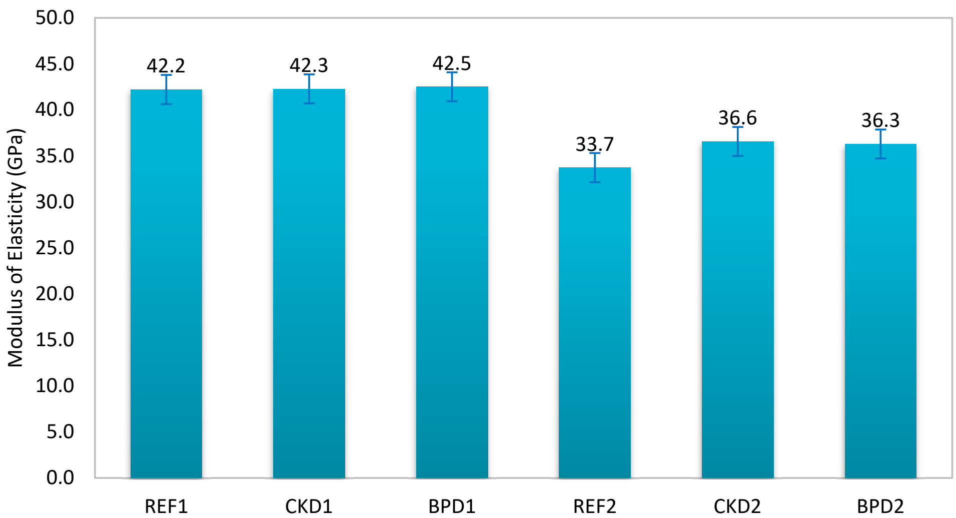

Figure 8. Modulus of Elasticity values of each SCC composition.

3.4. Tensile Splitting and Flexural Strength

Figures 9 and 10 provide useful information about the tensile splitting and the flexural strengths. The tensile-splitting test results of REF1 and BPD1 were almost identical, ranging between 3.0 and 3.1 MPa. The CKD1 composition had a slightly higher strength (3.4 MPa), a rather unexpected result, due to the high compressive strength of BPD concrete as well as the common upward trend between the compressive and the tensile strengths. This trend was confirmed, however, with the specimens of series 2, as the compositions REF2 and BPD2 reached the same tensile splitting strength (3.5 MPa), which again was lower than the corresponding strength of the CKD2 composition (3.9 MPa). This unusual trend could be attributed to the fineness of the CKD particles, in comparison with that of the

BPD particles, which forms an interfacial transitional zone of lower porosity and of denser microstructure [56]. The BPD1 and REF1 compositions achieved the highest and lowest flexural strengths of 5.4 MPa and 4.9 MPa, respectively, among the compositions of series 1, while the CKD1 mixture failed at approximately the same load as BPD1. Among the mixtures of series 2, REF2 also had the lowest flexural strength of 4.9 MPa, while BPD2 achieved the highest flexural strength of 6.7 MPa, following the compressive-strength trend given in Figure 6. What should be noted is that the flexural strength would probably have higher values; however, the specimens were not water-cured, but air-cured instead, in a curing chamber with constant conditions (24 °C, 65% RH), due to the drying-shrinkage monitoring test. However, useful conclusions can be drawn about the effect of each filler on the SCC bonding strength.

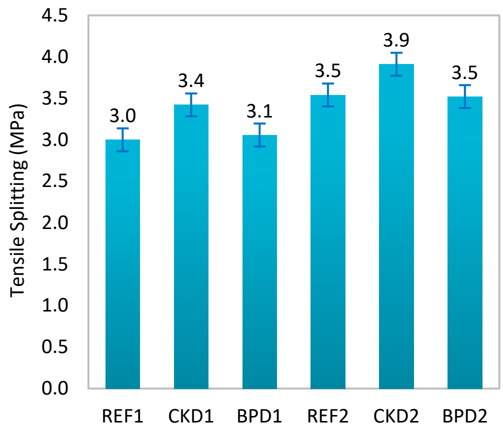

Figure 9. Tensile splitting strength of each SCC composition at the age of 90 days.

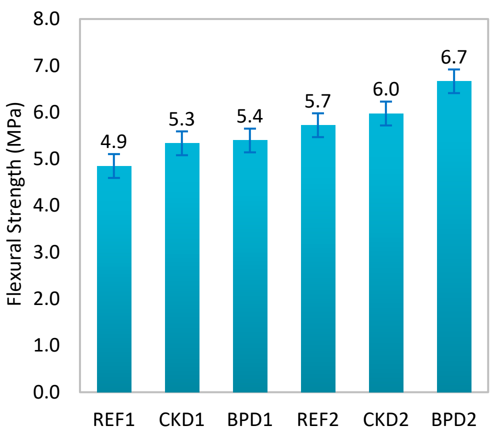

Figure 10. Flexural strength of each SCC composition at the age of 90 days.

The results of both the flexural and the tensile tests are very interesting, as the series 2 compositions in both cases achieved higher strengths, despite their lower compressive strength. This is attributed to the higher powder content (550 kg/m^3, instead of 500 kg/m^3) having a substantially beneficial effect on the microstructure of the interfacial transition zone, and the intrinsic quality of the matrix affecting the tensile strength of concrete [56].

3.5. Hardened Visual-Stability Index

In Figure 11, some representative photos of the specimens (one for each SCC composition) after splitting are presented. The hardened visual-stability indices (HVSIs) for all SCC bisected cylinders are equal to 0, confirming an SCC production of high stability without any signs of static segregation or bleeding. A visual observation of the cross-sections of Figure 11 confirms the aforementioned clearly, through the absence of any mortar or paste layer on the top of the specimens or any lengthwise difference in the distribution of the coarse aggregates, despite the action of the gravitational forces. These results are even more impressive for the specimens of series 2, considering that they contain more water and they are closer to the upper limit of the EFNARC Guidelines (210 kg/m^3) [3]. On the other hand, the high paste volume and high percentage of fine-powder content have a positive effect on the elimination of segregation phenomena [3]. Combining the HVSI with the sieve-segregation test results (Table 4), it is concluded that the specific SCC mixtures designed for the present study constitute stable mixtures of high cohesion, without showing any tendency toward segregation or bleeding.

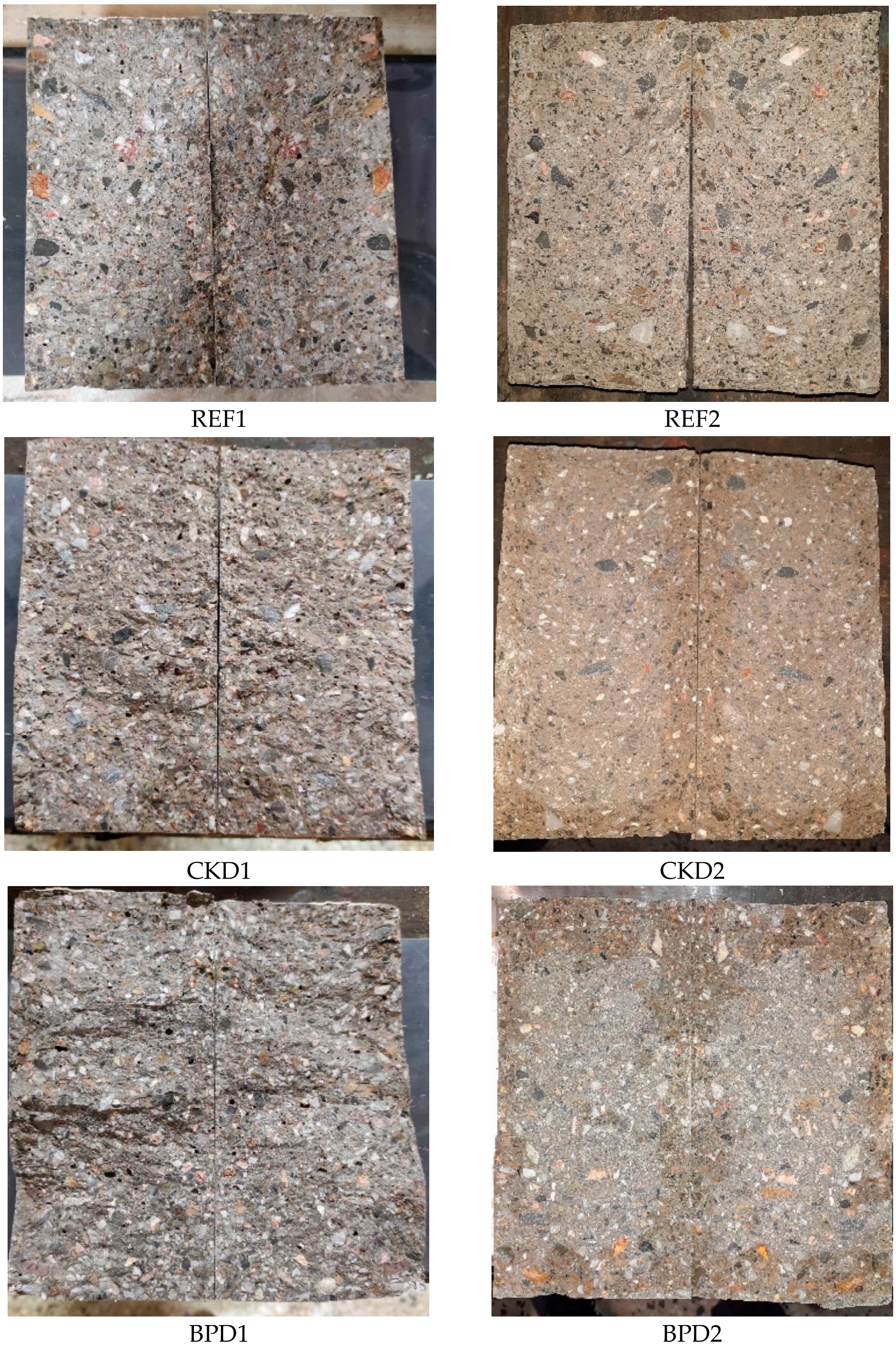

Figure 11. Indicative longitudinal sections of SCC cylindrical specimens.

3.6. Drying Shrinkage

Figure 12 shows the evolution of the drying shrinkage of each composition, at ages of 7, 14, 28 and 90 days, with respect to the corresponding limit for the drying shrinkage, as defined by the ACI 224R-01 [57]. REF2 is the only composition whose shrinkage marginally exceeded the above limit, registered with 28% greater values than REF1 after 90 days. This could be attributed to the increased w/c ratio and to the finer particles of the MP. It is known that by increasing the w/c ratio, the shrinkage increases, due to higher interconnected permeable voids and the lower values of modulus of elasticity [56], as shown in the Figure 8. Additionally, according to the literature [25], the fine particles of MP could act as a nucleation sites, advancing the hydration degree and enhancing the formation of the hydration products, which leads to a higher autogenous shrinkage, as well [19,58,59]. Nevertheless, the results of both the hydration heat [32] and the compressive strength (Figure 6) did not imply any significant differences between the samples as far as the hydration rate is concerned. Thus, only the higher w/c ratio could be considered to have affected the recorded shrinkage level.

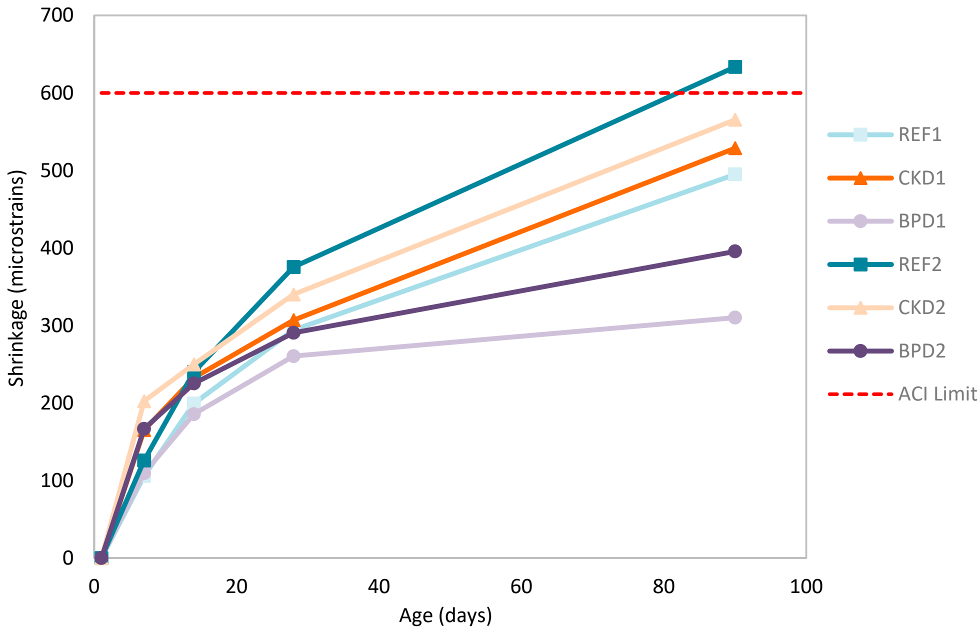

Figure 12. Free shrinkage for each SCC composition, measured at 7, 14, 28 and 90 days.

On the other hand, the mixtures containing CKD and BPD in the replacement of MP, showed a clear lower level of drying shrinkage. This improvement is attributed to the higher rate of compressive-strength development (Figure 6) and the higher values of the modulus of elasticity (Figure 8), both of which limit the deformation of the material. Furthermore, the high CaO content in BPD (Table 2) contributed to the reduced shrinkage of SCC, due to the carbonation associated with high contents of magnesium and calcium oxides [27,56,60,61]. The better performance of the mixture containing BPD, in comparison with CKD, could be also attributed to its coarser granulometry (Table 1). More specifically, the coarser granulometry (D90: 12.27 µm, 14.66 µm and 115.63 µm for MP, CKD and BPD, respectively) leads to lower capillary pressures, due to the coarser porous structure and the larger total specific surface area [19,27,62,63]. In addition, the VMA incorporation into SCC mixtures with BPD1 (Table 4) contributed to its volume stability and, therefore, to the lowest shrinkage (37% lower than REF1, after 90 days). VMA limits the water migration by bonding with water hydrogen, and reduces evaporation [62]. Finally, the highest SP dosage in compositions containing BPD (BPD1 and BPD2), compared to the other SCC mixtures, could also contribute slightly to the reduced drying shrinkage [64].

Figure 13 summarizes the correlation between air content, measured in fresh concrete mixtures and shrinkage, measured after 90 days of drying, showing a positive correlation between these properties. This correlation trend is influenced by the porous microstructure of the interfacial transition zone between cement paste and aggregates, as well as by the overlapping or interconnection between the pores that they were formed by the entrapped air. Moreover, the increased air content and the permeable voids lead to an increase in the vapor diffusion in SCC, which accelerates the water loss and, ultimately, the drying shrinkage [65].

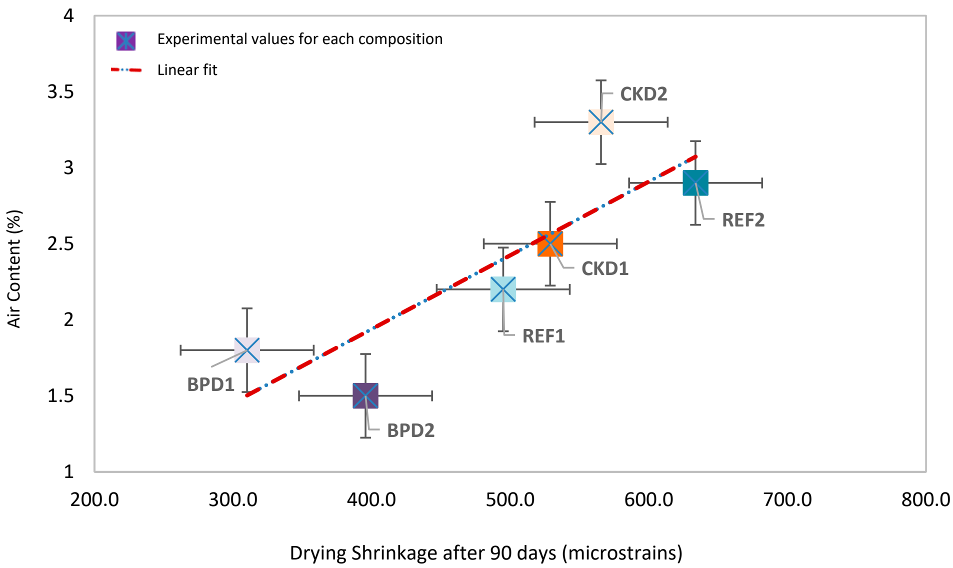

Figure 13. Correlation between drying shrinkage after 90 days and air content in the fresh SCC mixtures.

As presented in Figure 14, BPD1 underwent a 1.12% mass loss, by far the lowest compared to the other compositions, which had almost double mass losses, with percentages ranging from 1.92% for REF1 to 2.01% for CKD1. These results are directly related to the measured drying shrinkage (Figure 14). As expected, the prisms of series 2 showed higher percentages of mass loss, as they have more water to lose in their composition. In these series also, the mixture containing BPD had the lowest mass loss (1.44%), while REF2 and CKD2 had the highest mass-loss values, with 2.96% and 2.11%, respectively.

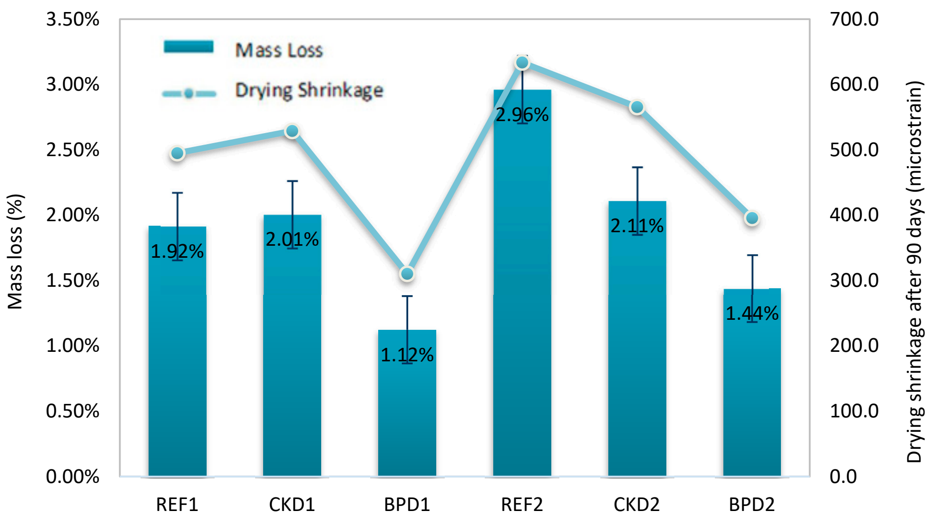

Figure 14. Mass loss and drying shrinkage for each SCC composition after 90 days of drying at 65% RH and 23 °C.

4. Conclusions

The incorporation of alternative fine-filler materials as a partial replacement for common limestone fillers like MP, led to the production of SCC mixtures of low cement content with satisfactory rheological and mechanical properties. In summary, this study contributes to the following conclusions:

- BPD proves appropriate as a reactive alternative waste material, as it contributes to the development of excellent mechanical properties at any testing age, with a concurrently low drying shrinkage. The compressive strength was at least 50% higher than the corresponding strength of the reference compositions, and the drying shrinkage approximately 50% lower.
- BPD incorporation in the designed proportion increases the viscosity, creating a potential barrier for those applications that require low-viscosity SCCs, while a higher SP dosage is also required to reach a yield stress equal to other compositions. Therefore, SCC compositions in the present study containing BPD are particularly well-suited for slightly reinforced structures (e.g., slabs), for casting through pump-injection systems (e.g., tunnel linings) or for smaller sections that prevent long horizontal flow (e.g., piles, foundations), as specified in the EFNARC guidelines. Nevertheless, specific investigation and parametric analysis will disclose the effect of BPD on the rheological behavior of SCC, and define its finest content for optimal performance.
- The addition of CKD to the SCC constitutes a potential sustainable solution, as it improves the compressive strength and drying shrinkage, and substantially improves the tensile strength, by almost 15%.
- At the same time, partially replacing MP with CKD contributes to more-than-acceptable rheological properties, achieving the desirable slump flow with 20–30% less SP than BPD. Thus, CKD proves to be a sufficient filler for SCCs intended for normal applications such as reinforced concrete walls, columns and beams.
- Testing the durability (e.g., chloride diffusion, water permeability carbonation resistance, corrosion resistance, alkali–silica reaction, etc.) of SCCs containing the alternative fillers that were studied in this work is a critical topic of high interest for future research. To ensure sufficient durability in the face of chemical challenges posed by alkalis, sulphates, and chlorides, it is strongly recommended to consider incorporating SCMs such as fly ash, silica fume, metakaolin, etc., in combination with cement, MP and CKD or BPD, in quaternary powder mixtures.

Author Contributions: Conceptualization, A.K., E.B. and I.M.; methodology, A.K., E.B. and K.S.; validation, A.K. and E.B.; formal analysis, A.K.; investigation, A.K.; writing—original draft, A.K.; writing—review and editing, A.K., E.B., K.S. and S.A.; visualization, A.K.; supervision, E.B.; project administration, A.K. and E.B. All authors have read and agreed to the published version of the manuscript.

Funding: This research received no external funding.

Institutional Review Board Statement: Not applicable.

Informed Consent Statement: Not applicable.

Data Availability Statement: The data presented in this study are available on request from the corresponding author.

Acknowledgments: The authors would like to sincerely thank the technical staff of all the involved NTUA laboratories (Civil Engineering, Mining and Metallurgical Engineering and Chemical Engineering). Special thanks are also due to Titan S.A. and Dionyssomarble S.A., who kindly provided the necessary materials.

Conflicts of Interest: Authors Stelios Antiohos and Ioannis Marinos were employed by the TITAN Cement Company S.A. The remaining authors declare that the research was conducted in the absence of any commercial or financial relationships that could be construed as a potential conflict of interest.

References

1. Khayat, K.; De Schutter, G. *Mechanical Properties of Self-Compacting Concrete, State-of-the-Art Report of the RILEM Technical Committee 228-MPS on the Mechanical Properties of Self-Compacting Concrete*; Springer: Cham, Switzerland, 2014.
2. Biricik, Ö.; Mardani, A. Parameters Affecting Thixotropic Behavior of Self Compacting Concrete and 3D Printable Concrete; a State-of-The-Art Review. *Constr. Build. Mater.* **2022**, *339*, 127688. [CrossRef]
3. The European Project Group. *The European Guidelines for Self-Compacting Concrete*; The European Project Group: Brussels, Belgium, 2005; Volume 63.
4. Ting, T.Z.H.; Rahman, M.E.; Lau, H.H.; Ting, M.Z.Y. Recent Development and Perspective of Lightweight Aggregates Based Self-Compacting Concrete. *Constr. Build. Mater.* **2019**, *201*, 763–777. [CrossRef]
5. Łaźniewska-Piekarczyk, B. The Influence of Admixtures Type on the Air-Voids Parameters of Non-Air-Entrained and Air-Entrained High Performance SCC. *Constr. Build. Mater.* **2013**, *41*, 109–124. [CrossRef]
6. Elyamany, H.E.; Abd Elmoaty, A.E.M.; Mohamed, B. Effect of Filler Types on Physical, Mechanical and Microstructure of Self Compacting Concrete and Flow-Able Concrete. *Alex. Eng. J.* **2014**, *53*, 295–307. [CrossRef]
7. Gupta, N.; Siddique, R.; Belarbi, R. Sustainable and Greener Self-Compacting Concrete Incorporating Industrial By-Products: A Review. *J. Clean. Prod.* **2021**, *284*, 124803. [CrossRef]
8. Meko, B.; Ighalo, J.O.; Ofuyatan, O.M. Enhancement of Self-Compactability of Fresh Self-Compacting Concrete: A Review. *Clean. Mater.* **2021**, *1*, 100019. [CrossRef]
9. Hameed, A.; Rasool, A.M.; Ibrahim, Y.E.; Afzal, M.F.U.D.; Qazi, A.U.; Hameed, I. Utilization of Fly Ash as a Viscosity-Modifying Agent to Produce Cost-Effective, Self-Compacting Concrete: A Sustainable Solution. *Sustainability* **2022**, *14*, 11559. [CrossRef]
10. Benjeddou, O.; Soussi, C.; Jedidi, M.; Benali, M. Experimental and Theoretical Study of the Effect of the Particle Size of Limestone Fillers on the Rheology of Self-Compacting Concrete. *J. Build. Eng.* **2017**, *10*, 32–41. [CrossRef]
11. Mathews, M.E.; Kiran, T.; Nammalvar, A.; Anbarasu, M.; Kanagaraj, B.; Andrushia, D. Evaluation of the Rheological and Durability Performance of Sustainable Self-Compacting Concrete. *Sustainability* **2023**, *15*, 4212. [CrossRef]
12. de Souza, A.M.; Franco de Carvalho, J.M.; Santos, C.F.R.; Ferreira, F.A.; Pedroti, L.G.; Peixoto, R.A.F. On the Strategies to Improve the Eco-Efficiency of Self-Compacting Concrete Using Industrial Waste: An Analytical Review. *Constr. Build. Mater.* **2022**, *347*, 128634. [CrossRef]
13. Ahmad, J.; Tufail, R.F.; Aslam, F.; Mosavi, A.; Alyousef, R.; Faisal Javed, M.; Zaid, O.; Khan Niazi, M.S. A Step towards Sustainable Self-Compacting Concrete by Using Partial Substitution of Wheat Straw Ash and Bentonite Clay instead of Cement. *Sustainability* **2021**, *13*, 824. [CrossRef]
14. Ahmad, J.; Abid, S.R.; Arbili, M.M.; Majdi, A.; Hakamy, A.; Deifalla, A.F. A Review on Sustainable Concrete with the Partially Substitutions of Silica Fume as a Cementitious Material. *Sustainability* **2022**, *14*, 12075. [CrossRef]
15. Pang, L.; Liu, Z.; Wang, D.; An, M. Review on the Application of Supplementary Cementitious Materials in Self-Compacting Concrete. *Crystals* **2022**, *12*, 180. [CrossRef]
16. Shah, S.A.R.; Ahmad, H.; Alhazmi, H.; Anwar, M.K.; Iqbal, F. Utilization of Self-Consolidated Green Material for Sustainable Development: An Environment Friendly Waste Materials Application for Circular Economy. *Polymers* **2021**, *13*, 2985. [CrossRef] [PubMed]
17. Siddique, R.; Kunal; Mehta, A. *Utilization of Industrial By-Products and Natural Ashes in Mortar and Concrete Development of Sustainable Construction Materials*; Elsevier Ltd.: Amsterdam, The Netherlands, 2019. [CrossRef]
18. Al-Bakri, A.Y.; Ahmed, H.M.; Hefni, M.A. Cement Kiln Dust (CKD): Potential Beneficial Applications and Eco-Sustainable Solutions. *Sustainability* **2022**, *14*, 7022. [CrossRef]
19. Wang, D.; Shi, C.; Farzadnia, N.; Shi, Z.; Jia, H. A Review on Effects of Limestone Powder on the Properties of Concrete. *Constr. Build. Mater.* **2018**, *192*, 153–166. [CrossRef]
20. Sfikas, I.P.; Badogiannis, E.G.; Trezos, K.G. Rheology and Mechanical Characteristics of Self-Compacting Concrete Mixtures Containing Metakaolin. *Constr. Build. Mater.* **2014**, *64*, 121–129. [CrossRef]
21. Abukhashaba, M.I.; Mostafa, M.A.; Adam, I.A. Behavior of Self-Compacting Fiber Reinforced Concrete Containing Cement Kiln Dust. *Alex. Eng. J.* **2014**, *53*, 341–354. [CrossRef]
22. Siddique, R. Utilization of Cement Kiln Dust (CKD) in Cement Mortar and Concrete-an Overview. *Resour. Conserv. Recycl.* **2006**, *48*, 315–338. [CrossRef]
23. Bagheri, S.M.; Koushkbaghi, M.; Mohseni, E.; Koushkbaghi, S.; Tahmouresi, B. Evaluation of Environment and Economy Viable Recycling Cement Kiln Dust for Use in Green Concrete. *J. Build. Eng.* **2020**, *32*, 101809. [CrossRef]
24. Maslehuddin, M.; Al-Amoudi, O.S.B.; Rahman, M.K.; Ali, M.R.; Barry, M.S. Properties of Cement Kiln Dust Concrete. *Constr. Build. Mater.* **2009**, *23*, 2357–2361. [CrossRef]
25. Najim, K.B.; Mahmod, Z.S.; Atea, A.K.M. Experimental Investigation on Using Cement Kiln Dust (CKD) as a Cement Replacement Material in Producing Modified Cement Mortar. *Constr. Build. Mater.* **2014**, *55*, 5–12. [CrossRef]
26. Rodríguez Viacava, I.; Aguado De Cea, A.; Rodríguez De Sensale, G. Self-Compacting Concrete of Medium Characteristic Strength. *Constr. Build. Mater.* **2012**, *30*, 776–782. [CrossRef]
27. Ashteyat, A.M.; Haddad, R.H.; Obaidat, Y.T. Case Study on Production of Self Compacting Concrete Using White Cement by Pass Dust. Case Stud. *Constr. Mater.* **2018**, *9*, e00190. [CrossRef]

28. Kounadis, A.; Tsivolas, K.; Badogiannis, E. Effect of By-Pass Filter Dust on Durability of Self-Compacting Concrete. *Mater. Proc.* **2023**, *15*, 26. [CrossRef]
29. *BS EN 12620:2013*; Aggregates for Concrete. British Standards Institution: London, UK, 2013.
30. *BS EN 197-1:2011*; Cement. Composition, Specifications and Conformity Criteria for Common Cements. British Standards Institution: London, UK, 2011.
31. *BS EN 934-2:2009*; Admixtures for Concrete, Mortar and Grout—Concrete Admixtures. Definitions, Requirements, Conformity, Marking and Labelling. British Standards Institution: London, UK, 2009.
32. Kounadis, A.; Badogiannis, E.G.; Retsa, N.; Angelopoulos, P.M.; Marinos, I. Hydration Heat, Rheology and Strength of Self-Compacting Sustainable Mortars Containing Alternative Filler Materials. *J. Mater. Civ. Eng.* **2022**, *34*, 1–10. [CrossRef]
33. *ASTM B923-02:2002*; Standard Test Method for Metal Powder Skeletal Density by Helium or Nitrogen Pycnometry. ASTM International: West Conshohocken, PA, USA, 2002. Available online: www.astm.org (accessed on 1 January 2023).
34. *BS ISO 13320:2009*; Particle size analysis. Laser diffraction methods (British Standard). British Standards Institution: London, UK, 2009.
35. *BS EN 12350-8:2010*; Testing Fresh Concrete—Part 8: Slump-Flow Test. British Standards Institution: London, UK, 2010.
36. *BS EN 12350-9:2010*; Testing Fresh Concrete—Part 9: V-Funnel Test. British Standards Institution: London, UK, 2010.
37. *BS EN 12350-11:2010*; Testing Fresh Concrete—Part 11: Sieve Segregation Test. British Standards Institution: London, UK, 2010.
38. *BS EN 12350-10:2010*; Testing Fresh Concrete—Part 10: L Box Test. British Standards Institution: London, UK, 2010.
39. *UNI 11044:2003*; Testing Fresh Self Compacting Concrete—Determination of Confined Flowability in U-Shape Box. Ente Nazionale Italiano di Unificazione (UNI): Milan, Italy, 2003.
40. *BS EN 12350-6:2009*; Testing Fresh Concrete—Part 6: Density. British Standards Institution: London, UK, 2009.
41. *BS EN 12350-7:2009*; Testing Fresh Concrete—Part 7: Air Content—Pressure Methods. British Standards Institution: London, UK, 2009.
42. *BS EN 12390-3:2009*; Testing Hardened Concrete—Part 3: Compressive Strength of Test Specimens. British Standards Institution: London, UK, 2009.
43. *BS EN 12390-6:2010*; Testing Hardened Concrete—Part 6: Tensile Splitting Strength of Test Specimens. British Standards Institution: London, UK, 2010.
44. *ASTM C469/C469M-14e1*; Standard Test Method for Static Modulus of Elasticity and Poisson's Ratio of Concrete in Compression. ASTM International: West Conshohocken, PA, USA, 2014. Available online: www.astm.org (accessed on 1 January 2023).
45. Illinois Test Procedure SCC-6. *Standard Test Method for Static Segregation of Hardened Self-Consolidating Concrete Cylinders*; Illinois Department of Transportation: Illinois, USA, 2007.
46. *BS EN 12390-16:2019*; Testing Hardened Concrete—Part 16: Determination of the Shrinkage of Concrete. British Standards Institution: London, UK, 2019.
47. *BS EN 12390-5:2009*; Testing Hardened Concrete—Part 5: Flexural Strength of Test Specimens. British Standards Institution: London, UK, 2009.
48. Tzouvalas, G.; Dermatas, N.; Tsimas, S. Alternative Calcium Sulfate-Bearing Materials as Cement Retarders: Part I. *Anhydrite. Cem. Concr. Res.* **2004**, *34*, 2113–2118. [CrossRef]
49. Shoaib, M.M.; Balaha, M.M.; Abdel-Rahman, A.G. Influence of Cement Kiln Dust Substitution on the Mechanical Properties of Concrete. *Cem. Concr. Res.* **2000**, *30*, 371–377. [CrossRef]
50. Elgalhud, A.A.; Dhir, R.K.; Ghataora, G. Limestone Addition Effects on Concrete Porosity. *Cem. Concr. Compos.* **2016**, *72*, 222–234. [CrossRef]
51. Siddique, R.; Gupta, N. Limestone Dust. In *Sustainable Concrete Made with Ashes and Dust from Different Sources*; Elsevier: Amsterdam, The Netherlands, 2021. [CrossRef]
52. Lea, F.M. *The Chemistry of Cement and Concrete*; Edward Arnold Ltd.: London, UK, 1970; p. 1092.
53. Singh, N.B.; Bhattacharjee, K.N.; Shukla, A.K. Effect of Alkali Bypass Dust on the Hydration of Granulated Blast Furnace Slag Blended Cement. *Cem. Concr. Res.* **1995**, *25*, 883–892. [CrossRef]
54. Fantous, T.; Yahia, A. Effect of HRWR-VMA-AEA Combinations and Shear on Air-Void Characteristics in Self-Consolidating Concrete. *Constr. Build. Mater.* **2020**, *253*, 119192. [CrossRef]
55. Craeye, B.; Van Itterbeeck, P.; Desnerck, P.; Boel, V.; De Schutter, G. Modulus of Elasticity and Tensile Strength of Self-Compacting Concrete: Survey of Experimental Data and Structural Design Codes. *Cem. Concr. Compos.* **2014**, *54*, 53–61. [CrossRef]
56. Mehta, P.K.; Monteiro, P.J.M. *Concrete: Microstructure, Properties, and Materials*, 4th ed.; McGraw-Hill Education: New York, NY, USA, 2014.
57. *ACI 224R-01*; Control of Cracking in Concrete Structures. American Concrete Institute: Farmington Hills, Michigan, USA, 2001.
58. Tang, S.; Huang, D.; He, Z. A Review of Autogenous Shrinkage Models of Concrete. *J. Build. Eng.* **2021**, *44*, 103412. [CrossRef]
59. Alrifai, A.; Aggoun, S.; Kadri, A.; Kenai, S.; Kadri, E. Paste and Mortar Studies on the Influence of Mix Design Parameters on Autogenous Shrinkage of Self-Compacting Concrete. *Constr. Build. Mater.* **2013**, *47*, 969–976. [CrossRef]
60. Abdalhmid, J.M.; Ashour, A.F.; Sheehan, T. Long-Term Drying Shrinkage of Self-Compacting Concrete: Experimental and Analytical Investigations. *Constr. Build. Mater.* **2019**, *202*, 825–837. [CrossRef]

61. Choudhary, R.; Gupta, R.; Alomayri, T.; Jain, A.; Nagar, R. Permeation, Corrosion, and Drying Shrinkage Assessment of Self-Compacting High Strength Concrete Comprising Waste Marble Slurry and Fly Ash, with Silica Fume. *Structures* **2021**, *33*, 971–985. [CrossRef]
62. Valcuende, M.; Marco, E.; Parra, C.; Serna, P. Influence of Limestone Filler and Viscosity-Modifying Admixture on the Shrinkage of Self-Compacting Concrete. *Cem. Concr. Res.* **2012**, *42*, 583–592. [CrossRef]
63. Mao, Y.; Liu, J.; Shi, C. Autogenous Shrinkage and Drying Shrinkage of Recycled Aggregate Concrete: A Review. *J. Clean. Prod.* **2021**, *295*, 126435. [CrossRef]
64. Sardinha, M.; de Brito, J.; Rodrigues, R. Durability Properties of Structural Concrete Containing Very Fine Aggregates of Marble Sludge. *Constr. Build. Mater.* **2016**, *119*, 45–52. [CrossRef]
65. Piasta, W.; Sikora, H. Effect of Air Entrainment on Shrinkage of Blended Cements Concretes. *Constr. Build. Mater.* **2015**, *99*, 298–307. [CrossRef]